

Absorption spectroscopy of xenon and ethylene–noble gas mixtures at high pressure: towards Bose–Einstein condensation of vacuum ultraviolet photons

Christian Wahl¹ · Rudolf Brausemann¹ · Julian Schmitt¹ · Frank Vewinger¹ · Stavros Christopoulos¹ · Martin Weitz¹

Received: 1 August 2016 / Accepted: 4 November 2016 / Published online: 2 December 2016
© Springer-Verlag Berlin Heidelberg 2016

Abstract Bose–Einstein condensation is a phenomenon well known for material particles as cold atomic gases, and this concept has in recent years been extended to photons confined in microscopic optical cavities. Essential for the operation of such a photon condensate is a thermalization mechanism that conserves the average particle number, as in the visible spectral regime can be realized by subsequent absorption re-emission processes in dye molecules. Here we report on the status of an experimental effort aiming at the extension of the concept of Bose–Einstein condensation of photons towards the vacuum ultraviolet spectral regime, with gases at high-pressure conditions serving as a thermalization medium for the photon gas. We have recorded absorption spectra of xenon gas at up to 30 bar gas pressure of the $5p^6-5p^56s$ transition with a wavelength close to 147 nm. Moreover, spectra of ethylene noble gas mixtures between 158 and 180 nm wavelength are reported.

1 Introduction

For now approaching 50 years, Theodor Hänsch has revolutionized spectroscopy by the use of lasers. One of the authors (M.W.) had the opportunity to carry out both his

doctorate and his habilitation degree work in Theodor Hänsch's laboratory at the Max-Planck-Institute of Quantum Optics near Munich. It is a pleasure to devote this article to Theodor Hänsch on the occasion of his 75th birthday.

For bosonic particles with a nonvanishing rest mass Bose–Einstein condensation to a macroscopically occupied ground state minimizes the free energy when cooled to very low temperature given a sufficient particle density [1–4]. In distinct contrast, Bose–Einstein condensation usually does not occur for photons [5]. For the perhaps most widely discussed photon gas, blackbody radiation [6, 7], photons disappear in the system walls when cooled to low temperature instead of exhibiting condensation to the ground mode. This is what is expressed by the common statement of the chemical potential vanishing for the photon case. Early theory work has proposed photon Bose–Einstein condensation in Compton scattering of X-rays [8], and Chiao et al. proposed a photon fluid in a nonlinear cavity [9, 10]. More recently, Bose–Einstein condensation of exciton–polaritons, which are mixed states of matter and light in the strongly coupled regime, has been observed experimentally in several groups [11–13]. Collisions of the material part of the polaritons here drive the system into or near thermal equilibrium.

Our group has in 2010 observed Bose–Einstein condensation of photons in a dye-solution-filled microcavity [14–16], a result confirmed more recently by Marelic and Nyman [17]. A cavity with very small mirror spacing here imprints a low-frequency cut-off for photons in the visible spectral range, yielding a range of allowed photon frequencies well above the thermal energy in frequency units. The confinement results in the photon gas becoming two-dimensional, with the longitudinal modal quantum number being frozen.

Thermalization of the cavity photons is achieved by repeated absorption re-emission processes by the dye

This article is part of the topical collection “Enlightening the World with the Laser” - Honoring T. W. Hänsch guest edited by Tilman Esslinger, Nathalie Picqué, and Thomas Udem.

✉ Martin Weitz
weitz@uni-bonn.de
Christian Wahl
wahl@iap.uni-bonn.de

¹ Institut für Angewandte Physik, Universität Bonn, Wegelerstraße 8, 53115 Bonn, Germany

molecules, equilibrating the photon gas to the rovibrational temperature of the dye, which is at room temperature. The dye molecules here fulfil the Kennard–Stepanov relation, a thermodynamic Boltzmann-type frequency scaling between absorption and emission spectra well known to apply for systems with both upper and lower electronic states rovibrational manifolds in thermal equilibrium [18–20], as here achieved from frequent collisions with solvent molecules in the dye solution. When the thermalization of the photon gas is faster than photon loss through, e.g. the cavity mirrors, photons condense into the macroscopically occupied mode at the position of the low-frequency cut-off on top of a spectrally broad thermal photon cloud. The opposite limit of photons leaving the cavity before they have a chance to thermalize, corresponds to the usual laser case [21, 22].

In contrast to a usual laser in a photon Bose–Einstein condensation set-up, no inverted active medium is required to generate coherent optical emission, and spontaneous emission is retrapped [14]. This makes the system particularly attractive for ultraviolet or vacuum ultraviolet coherent optical sources, a spectral regime at which inversion, and correspondingly laser operation, is hard to achieve. We are aware of ongoing other work aiming at high optical frequency coherent emission using quantum interference effects, forming “lasers without inversion” [23, 24]. A possible suitable medium for photon thermalization in the vacuum ultraviolet regime could be high-pressure noble gas samples, which exhibit electronic transitions starting from the electronic ground state in this spectral regime, or both mixtures between atoms or molecules and noble gases. Alkali–noble gas collisions are long known to be extremely elastic [25, 26], and for the case of rubidium–argon gas mixtures at a few 100 bar of argon pressure the applicability of the thermodynamic Kennard–Stepanov scaling between absorption and emission has been validated for the visible rubidium D-lines [27]. The latter results can be well described by a simple model that assumes equilibrium between external degrees of freedom and the internal structure of alkali–noble gas quasi-molecules in the electronic ground and excited state manifolds, as due to the frequent collisions in the dense buffer gas system. For the case of xenon noble gas, vacuum ultraviolet absorption spectra have in earlier work been carried out up to 20 bar pressure [28]. For simple molecules, a large collection of both absorption and partly also emission data exists in the vacuum ultraviolet spectral regime, but mostly only for pure samples or at moderate buffer gas pressures [29–31].

As a first step towards a photon condensate in the vacuum ultraviolet spectral regime, we have started experiments to test for the applicability of the Kennard–Stepanov relation of gas samples, to provide a spectroscopic test of possible photon gas thermalization. Using the emission of a VUV deuterium lamp, we have recorded absorption spectra

of xenon gas in the 142–160 nm wavelength range for up to 30 bar of pressure. Moreover, spectra of ethylene molecules have been recorded in the 155–180 nm wavelength range for up to 130 bar of argon buffer gas pressure.

A further motivation for the here described work stems from the possibility to carry out collisional redistribution laser cooling of the dense gas samples. In earlier work of our group, collisional laser cooling has been carried out with rubidium gases subject to near 200 bar argon buffer gas pressure, where frequent rubidium–argon collisions shift the alkali atomic transition into resonance with a far-red-detuned laser beam, while spontaneous decay occurs near the unperturbed resonance frequency [32, 33]. The reaching of a sufficient alkali vapour pressure near 1 mbar here requires for a preheating of the sample cells, while gases that are gaseous at room temperatures, as ethylene, CO₂ or pure noble gases, could allow for redistribution laser cooling starting from room temperature conditions. The electronic transitions of such gases frequently are in the ultraviolet or vacuum ultraviolet spectral regime, as investigated in the here described work.

In the following, Sect. 2 describes the used experimental set-up, and Sect. 3 gives obtained spectroscopic data for the case of xenon gas. Further, in Sect. 4 we present results obtained with molecular ethylene gas both for the case without and with noble gas buffer gas. Finally, Sect. 5 gives conclusions.

2 Experimental set-up

A schematic of the used experimental apparatus for VUV absorption measurements is shown in Fig. 1a. The optical set-up including the high-pressure cell containing the investigated gas sample is placed in a vacuum chamber evacuated to 5×10^{-5} mbar. As a light source for the spectroscopy set-up we use a 200 W deuterium lamp (model: Heraeus D200VUV), whose optical emission spans the spectral range from 120 to 400 nm. Its emission is not uniform within this spectral range, but rather exhibits variations by two orders of magnitude, see Fig. 1b. Therefore, a two monochromator set-up is used, which allows for a large dynamic range of the spectroscopy signal. At first, a home-built grating monochromator (see Fig. 1a) provides initial wavelength selection of the source, which besides the enhancement of the possible dynamic range of the spectroscopy set-up also suppresses transitions in the gas sample driven by radiation with wavelength outside of the detection window. The home-built monochromator is equipped with a grating with 1200 groves/mm with a blaze angle optimized for 200 nm radiation. The concave grating focuses the emission to a first exit slit of 400 μm width. The width of spectral selection of this first

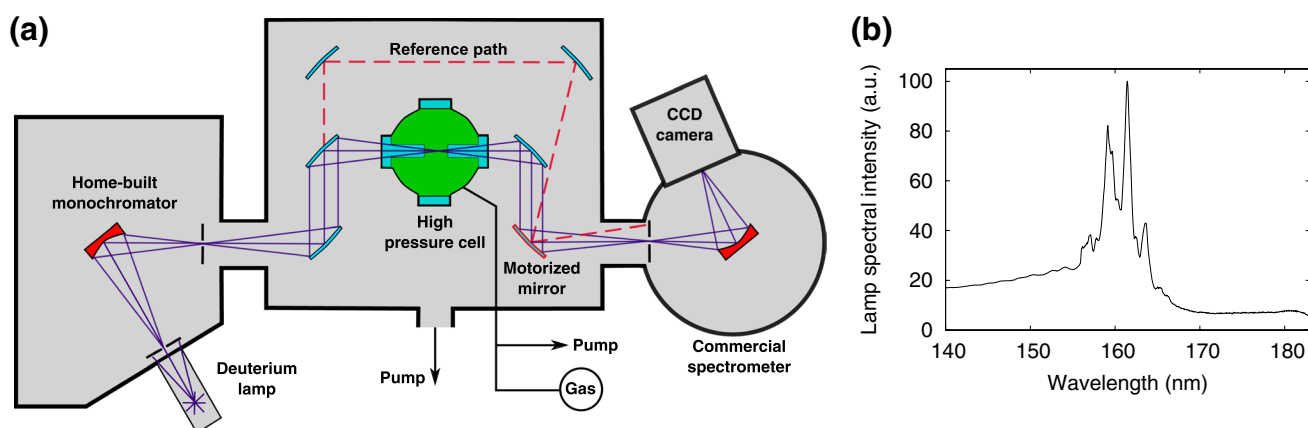


Fig. 1 **a** Schematic representation of the experimental set-up. Light emitted from the deuterium lamp is spectrally filtered by the first monochromator and sent through a high-pressure cell containing the gas to be analysed. A fraction of the light passes around the cell and is used to monitor the source output. A flip mirror is used to guide

light from one of the two paths into the detection spectrometer. All optical elements in this set-up are coated with aluminium and a protective magnesium difluoride (MgF_2) layer. **b** Deuterium source spectral intensity between 140 and 185 nm

monochromator is 2.2 nm. The spectrally filtered radiation is split into a reference and a measurement beam. The latter is focused into a high-pressure cell containing the sample and then directed onto a commercial grating spectrometer (model: McPherson 234/302) consisting of a 10- μm -wide entrance slit and a concave grating with 2400 lines/mm, which images the entrance slit onto an open nose VUV sensitive CCD camera. The spectral resolution of the commercial spectrometer is 0.05 nm. The reference beam is guided around the sample cell and by means of a motorized mirror can be, alternatively to the measurement beam, sent onto the commercial spectrometer. This allows for a normalization of the detected spectrum. This was done for each data point individually since we found the intensity of the detected signal to fluctuate over time by nearly 30% on a 30-min timescale, an issue that is most likely due to polarization variations of the source which lead to intensity changes by the used optical elements, e.g. from a polarization dependent reflectivity of the used mirrors.

The samples investigated in this work include high-purity ethylene, argon, helium, and xenon gases. High gas pressures, above 40 bar, are measured using a 200 bar gauge with a 1 bar resolution. Intermediate pressures in the range between 150 mbar and 40 bar are determined using a digital gauge with a 10 mbar resolution. For pressures below 150 mbar, a fine needle gauge is utilized, giving a resolution of 0.05 mbar. The pressure cell is constructed to house pressures of up to 200 bar. To ensure a largely contamination free environment, the high-pressure cell is repeatedly flushed with argon and evacuated to 10^{-5} mbar. Before each absorption measurement, a reference is taken to ensure that no residual absorption is observed. In order to seal the cell MgF_2 step windows of different step lengths

are used, which further allow to vary the absorption length in the cell.

To measure broadband absorption spectra both monochromators are first coupled, set to the same wavelength and subsequently scanned over the whole region of interest. Since the width of the spectral selection of the first monochromator is 2.2 nm, wavelength steps of 1 nm are performed while measuring the absorption and lamp output for each wavelength setting. The resulting signals are then, after being corrected for the current power of the deuterium lamp, used to create a spectrum spanning the region of interest. Broadband absorption spectra are then determined from the Lambert–Beer law.

3 Xenon VUV absorption measurements

To begin with, we have recorded xenon absorption spectra around the transition from the $5p^6$ ground state to the $5p^56s$ electronically excited state near 147 nm. At the used high xenon gas pressures frequent collisions between atoms occur and the quasi-molecular character in a regime beyond the impact limit determines the line shapes. Figure 2 shows calculated potential curves for the binary xenon system including the relevant levels. The lines in Fig. 3 show experimentally observed absorption data for various xenon pressures in the range of 0.1–30 bar. We observe significant pressure broadening, with the red wing being strongly enhanced with respect to the blue wing. This is well understood from the potential curves shown in Fig. 2, with the ground state for not too small internuclear distances being mostly flat and the excited state decreasing in energy. As the average internuclear distance decreases with increasing

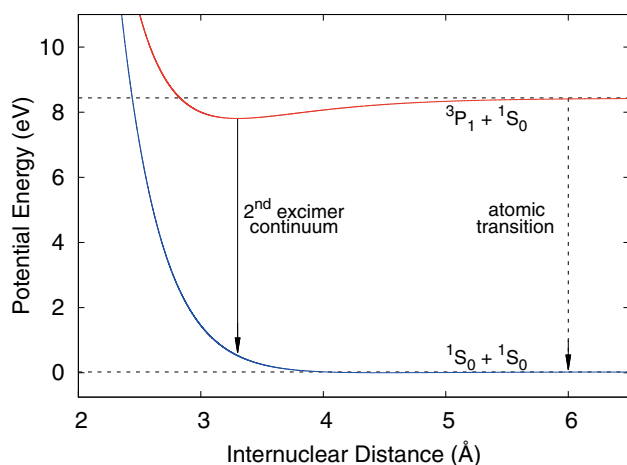


Fig. 2 Calculated energy in the xenon dimer system versus the internuclear distance [34, 35]. The horizontal dashed lines give the asymptotic energy levels for infinitely large internuclear distance

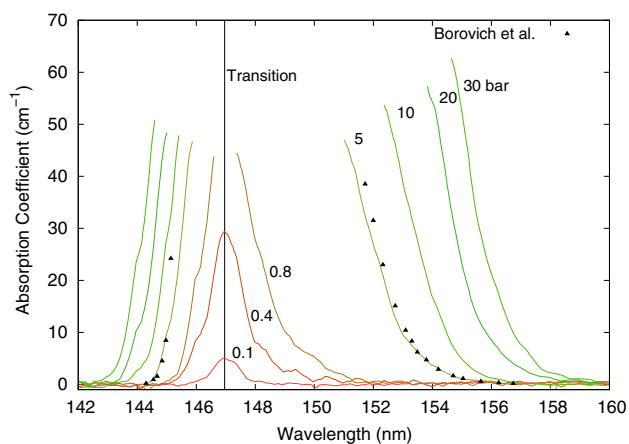


Fig. 3 Absorption coefficients of pure xenon in the wavelength range of 142–160 nm for pressures between 0.1 and 30 bar. Xenon pressures are indicated next to the respective absorption spectrum. Saturated regions are omitted for clarity, and the black triangles indicate comparable measurements from Borovich et al. for the 5 bar dataset [28]

pressure lower photon energies are sufficient to excite the transition, leading to an enhanced pressure broadening of the red wing with respect to that of the blue wing. Above a pressure of 0.4 bar, the absorption coefficient at the line centre cannot be resolved due to the here very high optical density. Correspondingly, we also cannot determine the linewidth for the high-pressure data, but already at the quoted pressure value of 0.4 bar the linewidth exceeds the thermal energy $k_B T$ in wavelength units of 0.5 nm at room temperature for a wavelength of 147 nm. Our results are in good agreement with earlier measurements by Borovich et al. [28], see the exemplary data points for a pressure of 5 bar in Fig. 3.

The spontaneous emission of the xenon system at pressures above 50 mbar, where the collision rate is sufficient that excimer molecules form faster than spontaneous decay, is known to be dominated by the second continuum around 172 nm, see the corresponding potential curve of Fig. 2. Though a linear extrapolation of our presented data with pressure does not indicate a significant overlap with emission at the second continuum at pressures below values reachable with our cell (200 bar), upon reaching of the critical pressure of 58.4 bar in the xenon system a highly nonlinear increase in the density with pressure does occur, which will strongly influence the spectra. This has been indicated in earlier narrowband optical measurements [36]. We are currently working on corresponding broadband measurements in this regime.

4 Absorption spectroscopy of ethylene

An alternative promising approach for a thermalization medium for a photon Bose–Einstein condensate in the VUV spectral regime are simple molecules in high-pressure noble buffer gas environments. Ethylene molecules show electronic transitions in the relevant wavelength range, and the low-pressure regime (below 0.3 mbar) of pure ethylene has previously been studied [29–31]. To begin with, we have investigated corresponding spectra of pure ethylene up to 20 mbar pressure in the wavelength range between 158 and 180 nm, see Fig. 4a. The absorption coefficient scales proportionally with increasing ethylene concentration as expected from Beer’s law, while no evident pressure-broadening effect can be observed. Earlier experiments are in very good agreement with the present work, presenting comparatively negligible discrepancies (on the order of 0.1 nm) in the observed peak positions. Figure 4b gives corresponding ethylene spectra both without (bottom) and with argon buffer gas, for buffer gas pressures of up to 130 bar. The ethylene molecular partial pressure here was 1 mbar. One observes that the addition of the buffer gas broadens the individual resonances, while the overall spectral structure is not significantly modified. Additionally, we observe for the three visible doublets with minima at 165.6, 168.4, and 173.5 nm, respectively, that the long wavelength peak is dominant at low buffer gas pressures compared to the short wavelength peak, which is inverted at high buffer gas pressures. When using helium instead of argon as a buffer gas no significant modification of the spectra is observed, see the exemplary curve in Fig. 4b.

To quantify the pressure broadening by the buffer gas we focus on the spectral peak near 174.1 nm. As we cannot unambiguously determine the width of this line due to the many nearby resonances and the asymmetry of the line shapes, we instead use a normalized doublet visibility

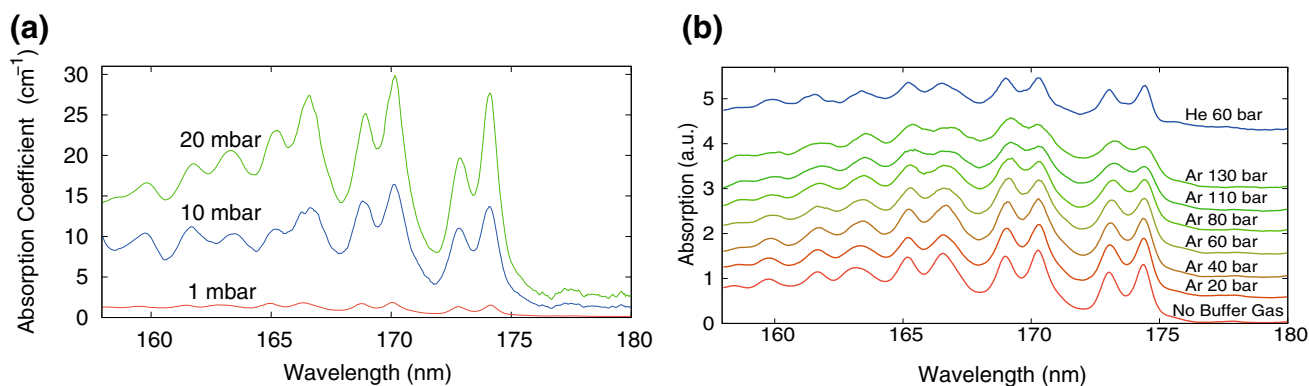


Fig. 4 **a** Absorption coefficients in the wavelength range of 158–180 nm for three different pressures of pure ethylene, 1 mbar (red), 10 mbar (blue), and 20 mbar (green). **b** Absorption spectra for 1 mbar of ethylene with the addition of 20–130 bar argon. Spectra are vertically shifted by 0.5 for clarity. It is observed that the peaks in the eth-

ylene spectrum experience a *red-shift* dependent on argon pressure. Further, a strong decrease in contrast between peak and underlying continuum is apparent. The *top* spectrum (blue line) gives an exemplary spectrum for helium buffer gas at 60 bar pressure

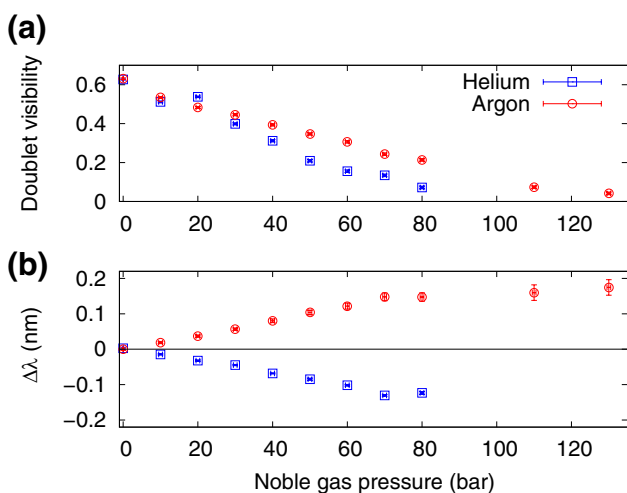


Fig. 5 **a** Extracted visibility doublet and **b** shift $\Delta\lambda$ of the position for the peak found at 174.1 nm in 1 mbar of ethylene with added argon (red circles) and helium (blue squares) buffer gas versus the noble gas pressure. While both noble gases lead to a similar change in visibility, an opposing effect can be seen with respect to the wavelength shift

$V = (\kappa_{\max} - \kappa_{\min}) / (\kappa_{\max} + \kappa_{\min})$, where κ_{\max} and κ_{\min} denote the absorption coefficients on resonance and at the minimum between the resonances of the doublet structure at 172.8 and 174.1 nm, respectively, to quantify the pressure broadening, see also Fig. 4b. The variation of the doublet visibility for both argon and helium buffer gas with pressure is shown in Fig. 5a. The data show that the loss of doublet visibility with pressure and correspondingly also the pressure broadening is somewhat larger for the case of helium than for argon buffer gas. Figure 5b shows the pressure-induced shift $\Delta\lambda$ of the 174.1 nm resonance for both

of the buffer gases, which has been obtained from a fit to the data of the resonance line. We observe a pressure shift of similar magnitude, but of opposite sign for the two noble gases. Similar effects have been reported in earlier works for other systems when using different noble gas perturbers and were attributed to the differing collisional kinetics of the gas mixtures [37, 38]. Here we find that for pressures of up to 60 bar the shift is linear to good approximation, with a slope of 0.1 nm per 50 bar, while for higher pressures a saturation of the shift is observed. At 130 bar argon buffer gas pressure, the observed pressure shift is 0.18 nm, corresponding to $0.29k_B T$ in wavelength units at room temperature for a wavelength of 174 nm. This shift is roughly a factor of eight smaller than the pressure broadening responsible for the above-discussed reduction in the visibility of the doublet spaced by 1.4 nm.

5 Conclusions and outlook

To conclude, we have presented absorption spectra of both xenon gas and binary mixtures of ethylene with noble gases at high pressure. Our measurements show a broadening of resonances of order of the thermal energy $k_B T$. For the case of the ethylene data, both the data with and without noble buffer gas can provide valuable input for future calculations of molecular potentials.

In the future, we plan to test for the thermodynamic Kennard–Stepanov scaling of the dense gas samples, for which additionally fluorescence spectra at the corresponding parameters are required. Besides the here presented xenon system, the lighter noble gases offer even shorter wavelength closed electronic transitions, as candidate systems for photon condensates in the deeper ultraviolet

spectral regime. Provided that the Kennard–Stepanov relation in the dense system holds, this implies a high quantum efficiency of the involved transitions [39]. Besides photon Bose–Einstein condensation, this would make the system also a promising candidate for collisional redistribution laser cooling starting from room temperature [32].

Acknowledgements We acknowledge support of the Deutsche Forschungsgemeinschaft (within SFB/TRR 185 and We1748-17) and the European Research Council (INPEC). We thank G. Wallstabe for his contributions in the early phase of this experiment.

References

1. A. Einstein, Zur Quantentheorie des idealen Gases. Sitz. ber. Preuss. Akad. der Wiss. **1**, 1–3 (1925)
2. E.A. Cornell, C.E. Wieman, Nobel lecture: Bose–Einstein condensation in a dilute gas, the first 70 years and some recent experiments. *Rev. Mod. Phys.* **74**, 875 (2002)
3. W. Ketterle, Nobel lecture: when atoms behave as waves: Bose–Einstein condensation and the atom laser. *Rev. Mod. Phys.* **74**, 1131 (2002)
4. M.H. Anderson, J.R. Ensher, M.R. Matthews, C.E. Wieman, E.A. Cornell, Observation of Bose–Einstein condensation in a dilute atomic vapor. *Science* **269**, 198 (1995)
5. K. Huang, *Statistical Mechanics*, 2nd edn. (Wiley, Hoboken, 1987)
6. M. Planck, On the law of distribution of energy in the normal spectrum. *Ann. Phys.* **4**, 1 (1901)
7. S.N. Bose, Plancks Gesetz und Lichtquantenhypothese. *Z. Phys.* **26**, 178 (1924)
8. Y.B. Zel'Dovich, E. Levich, Bose condensation and shock waves in photon spectra. *Sov. Phys. JETP* **28**, 11 (1969)
9. R.Y. Chiao, Bogoliubov dispersion relation for a “photon fluid”: is this a superfluid? *Opt. Commun.* **179**, 157 (2000)
10. E. Bolda, R. Chiao, W. Zurek, Dissipative optical flow in a nonlinear Fabry–Pérot cavity. *Phys. Rev. Lett.* **86**, 416 (2001)
11. J. Kasprzak et al., Bose–Einstein condensation of exciton polaritons. *Nature* **443**, 409 (2006)
12. H. Deng, H. Haug, Y. Yamamoto, Exciton–polariton Bose–Einstein condensation. *Rev. Mod. Phys.* **82**, 1489 (2010)
13. R. Balili, V. Hartwell, D. Snoke, L. Pfeiffer, K. West, Bose–Einstein condensation of microcavity polaritons in a trap. *Science* **316**, 1007 (2007)
14. J. Klaers, J. Schmitt, F. Vewinger, M. Weitz, Bose–Einstein condensation of photons in an optical microcavity. *Nature* **468**, 545 (2010)
15. J. Klaers, J. Schmitt, T. Damm, F. Vewinger, M. Weitz, Bose–Einstein condensation of paraxial light. *Appl. Phys. B* **105**, 17 (2011)
16. J. Schmitt, T. Damm, D. Dung, F. Vewinger, J. Klaers, M. Weitz, Observation of grand-canonical number statistics in a photon Bose–Einstein condensate. *Phys. Rev. Lett.* **112**, 030401 (2014)
17. J. Marelic, R. Nyman, Experimental evidence for inhomogeneous pumping and energy-dependent effects in photon Bose–Einstein condensation. *Phys. Rev. A* **91**, 033813 (2015)
18. E.H. Kennard, *Phys. Rev.* **11**, 29 (1918)
19. B. Stepanov, *Dokl. Akad. Nauk SSSR* **112**, 839 (1957)
20. D.A. Sawicki, R.S. Knox, Universal relationship between optical emission and absorption of complex systems: an alternative approach. *Phys. Rev. A* **54**, 4837 (1996)
21. P. Kirton, J. Keeling, Nonequilibrium model of photon condensation. *Phys. Rev. Lett.* **111**, 100404 (2013)
22. J. Schmitt, T. Damm, D. Dung, F. Vewinger, J. Klaers, M. Weitz, Thermalization kinetics of light: from laser dynamics to equilibrium condensation of photons. *Phys. Rev. A* **92**, 011602 (2015)
23. A. Zibrov, M. Lukin, D. Nikonov, L. Hollberg, M. Scully, V. Velichansky, H. Robinson, Experimental demonstration of laser oscillation without population inversion via quantum interference in Rb. *Phys. Rev. Lett.* **75**, 1499 (1995)
24. O. Kocharovskaya, Amplification and lasing without inversion. *Phys. Rep.* **219**, 175 (1992)
25. E. Speller, B. Staudenmayer, V. Kemper, Z. Phys., Quenching cross sections for alkali–inert gas collisions. *Z. Phys. A At. Nucl.* **291**, 311 (1979)
26. U. Vogl, M. Weitz, Spectroscopy of atomic rubidium at 500-bar buffer gas pressure: approaching the thermal equilibrium of dressed atom–light states. *Phys. Rev. A* **78**, 011401 (2008)
27. P. Moroshkin, L. Weller, A. Saß, J. Klaers, M. Weitz, Kennard–Stepanov relation connecting absorption and emission spectra in an atomic gas. *Phys. Rev. Lett.* **113**, 063002 (2014)
28. B. Borovich, V. Zuev, D. Stavrovsky, Pressure-induced ultraviolet absorption in rare gases: absorption coefficients for mixtures of Xe and Ar at pressures up to 40 atm in the vicinity of 147 nm. *J. Quant. Spectr. Radiat. Transf.* **13**, 1241 (1973)
29. H.C. Lu, H.K. Chen, B.M. Cheng, Analysis of C₂H₄ in C₂H₆ and C₂H₅D with VUV absorption spectroscopy and a method to remove C₂H₄ from C₂H₆ and C₂H₅D. *Anal. Chem.* **76**, 5965 (2004)
30. M. Zelikoff, K. Watanabe, Absorption coefficients of ethylene in the vacuum ultraviolet. *JOSA* **43**, 756 (1953)
31. V.L. Orkin, R.E. Huie, M.J. Kurylo, Rate constants for the reactions of OH with HFC-245cb (CH₃CF₂CF₃) and some fluoroalkenes (CH₂CHCF₃, CH₂CF₂CF₃, CF₂CF₂CF₃, and CF₂CF₂). *J. Phys. Chem. A* **101**, 9118 (1997)
32. U. Vogl, M. Weitz, Laser cooling by collisional redistribution of radiation. *Nature* **461**, 70 (2009)
33. S. Yeh, P. Berman, Theory of collisionally aided radiative excitation. *Phys. Rev. A* **19**, 1106 (1979)
34. O. Dutuit, M. Castex, J. Le Calve, M. Lavollee, Synchrotron radiation study of the molecular xenon fluorescence around 2000 Å. *J. Chem. Phys.* **73**, 3107 (1980)
35. K.K. Docken, T.P. Schafer, Spectroscopic information on ground-state Ar 2, Kr 2, and Xe 2 from interatomic potentials. *J. Mol. Spectrosc.* **46**, 454 (1973)
36. H.A. Koehler, L.J. Ferderber, D.L. Redhead, P.J. Ebert, Vacuum-ultraviolet emission from high-pressure xenon and argon excited by high-current relativistic electron beams. *Phys. Rev. A* **9**, 768 (1974)
37. C. Beer, R. Bernheim, Hyperfine pressure shift of Cs 133 atoms in noble and molecular buffer gases. *Phys. Rev. A* **13**, 1052 (1976)
38. N. Allard, J. Kielkopf, The effect of neutral nonresonant collisions on atomic spectral lines. *Rev. Mod. Phys.* **54**, 1103 (1982)
39. J. Klaers, The thermalization, condensation and flickering of photons. *J. Phys. B At. Mol. Opt.* **47**, 243001 (2014)